ISSN(PRINT) : 2320 -1967
ISSN(ONLINE) : 2320 -1975

GLOBAL SCIENTIFIC INC.

ChemXpress

ORIGINAL ARTICLE

CHEMXPRESS 8(2), 57-73, (2015)

A structural and vibrational investigation on a material for sodium-ion batteries, the NASICON-type $Na_3V_2(PO_4)_3$ compound based on *Ab-Initio* calculations

María J.Márquez, María B.Márquez, María F.Ladetto, Silvia A.Brandán*

Cátedra de Química General, Facultad de Bioquímica, Química y Farmacia, Universidad Nacional de Tucumán, Ayacucho 471, 4000, San Miguel de Tucumán, Tucumán, (ARGENTINA)
E- mail: sbrandan@fbqf.unt.edu.ar

Abstract : Here, a structural and vibrational investigation on a material for sodium-ion batteries, NASICON-type based on *Ab-Initio* calculations in gas and aqueous solution phases is reported. The increase of the molar volume for NASICON in solution justifies the higher mobility of the Na^+ ions in the three-dimensional framework. The NBO results shows the high stability of NASICON and their anion in both media while the AIM calculations reveals the nature ionic of both species. The gap energies evidence the higher reactivity of NASICON, as compared with their anion. The force fields, force constants and complete assignments for both species are reported.

Keywords : Nasicon, $Na_3V_2(PO_4)_3$; Vibrational spectra; Molecular structure; Force field; DFT calculations.

INTRODUCTION

In recent times, new works on the employ of Na Super Ionic Conductor (NASICON) type, $Na_3V_2(PO_4)_3$ as electrode in Sodium-Ion battery were reported[1-4]. Today, these batteries are used as alternatives to lithium-ion batteries for large-scale renewable energy storage units taking into account their low cost and the abundance of sodium bearing precursors in the earth's mineral deposits, as reported by Liu et al.[2]. The electrochemical properties of a similar compound $Na_3V_2(PO_4)(2)F^{-3}$ were published by Shakoor et al.[4] combining first principles calculations with experimental studies in order to elucidate the mechanisms of the structural evolution and the electrochemical behavior of those species. The crystal structure of trisodium divanadium(III) tris(orthophosphate), $Na_3V_2(PO_4)_3$ and their anion $[V_2(PO_4)_3]^{3-}$ were determinate by Zavtosky[3] by using X-ray diffraction but, so far, their structural and vibrational properties remain unsolved. Structurally, the PO_4 groups are tetrahedral in the framework $[V_2(PO_4)_3]^{3-}$ anion and, the mode of coordination adopted by these groups, in accordance with that experimental structure[3], is bidentate. This way, the structural and vibrational properties

ORIGINAL ARTICLE

together with the chemical reactivities of $Na_3V_2(PO_4)_3$ and their anion are directly related with the stereochemistry of these species. Actually, there are few data in the literature on the vibrational analyses of both species and to detect them by means of vibrational spectroscopy it is necessary to perform their complete assignments. In a spectroscopic study on phosphate-based electrodes for lithium rechargeable batteries (LISICON), a vibrational assignment for vibration stretching modes corresponding to the PO_4 groups of $Li_3V_2(PO_4)_3$ was reported from electrochemical point of view[6]. In this work, as part of studies associated with inorganic compounds containing transition metals and different monodentate and/or bidentate ligands[7-12], the $Na_3V_2(PO_4)_3$ compound and their anion were structural and vibrationally studied from a theoretical point of view by using the available infrared spectra reported in the literature[6] and the experimental data published for those two structures[5]. Both species were studied in gas and aqueous solution phases taking into account that the alkaline ions of the aqueous electrolyte can intercalate the $Na_3V_2(PO_4)_3$ electrode compound[1]. Hence, the aim of this work is to perform *Ab-initio* calculations in gas and aqueous solution phases in order to calculate the best level of theory and best basis set to reproduce the experimental structure and wavenumbers. Furthermore, with the optimized geometries for those two species the atomic charges, stabilization energies, solvation energies, bond orders, maps electrostatic potential and topological properties of the charge density were calculated and, the complete vibrational assignments of both species combining the normal coordinate analysis with the scaled quantum mechanical force field (SQMFF) methodology[13] were performed. For these purposes, the initial structures for $Na_3[V2(PO_4)_3]$ and their $[V_2(PO_4)_3]^{3-}$ anion in both media were optimized by using the HF, B3P86 and B3LYP levels of theory employing the Los Alamos LanL2DZ split-valence[14-16] and CEP-4G[17-19] basis sets. The self-consistent reaction field (SCRF) method was used to study the solvent effects taking into account the the integral equation formalism variant (IEFPCM) model[20]. In addition, the force fields for both species in the two media were reported and their corresponding reactivities were predicted by means of the frontier molecular HOMO and LUMO orbitals. Finally, the structural and topological properties and the force constants determinate for $Na_3[V2(PO_4)_3]$ and their $[V_2(PO_4)_3]^{3-}$ anion were analyzed and compared between them.

COMPUTATIONAL DETAILS

According to the objectives of this work, to a better reproduction of the experimental structure and wavenumbers of $Na_3[V2(PO_4)_3]$ the election of a adequate method and basis set is very important to evaluate the best method of calculation to be used. In this sense, for species containing transition metals, such as V or Cr[21-26], in general the DFT calculations are more satisfactory than the HF methods and, particularly, for chromium oxo anions and oxyhalides compounds Bell et al.[27] have published that the B3LYP/Lanl2DZ method gives the best levels approximations for the structures and vibrational spectra of these compounds. In this case, we have used the HF level of theory together with the hybrid B3P86 and B3LYP methods[28,29] employing the Los Alamos LanL2DZ split-valence[14-16] and CEP-4G[17-19] basis sets because for the V atom there are few basis sets defined. The initial structures for $Na_3[V2(PO_4)_3]$ and their $[V_2(PO_4)_3]^{3-}$ anion in gas and aqueous solution phases were those experimental ones determined by using X-ray diffraction[5] which, were first modelled with the *GaussView* program[30] and, later optimized with all those methods mentioned by using the Gaussian 09 program[31]. Figure 1 shows the structures and labelling of all the atoms for the two species optimized. In aqueous solution, the theoretical structures were simulated using the IEFPCM model[20] considering the cavity of series of spheres with the SCRF method while the solvation energy values were calculated by using the solvation model (SMD)[32], as implemented in the Gaussian 09 program[31]. Taking into account that in the lithium-ion batteries the effect of vanadium on the physicochemical and electrochemical properties are attributed to its open three-dimensional framework[33], as in the structures of $Na_3[V2(PO_4)_3]$ and their $[V_2(PO_4)_3]^{3-}$ anion, for these two species is of

ORIGINAL ARTICLE

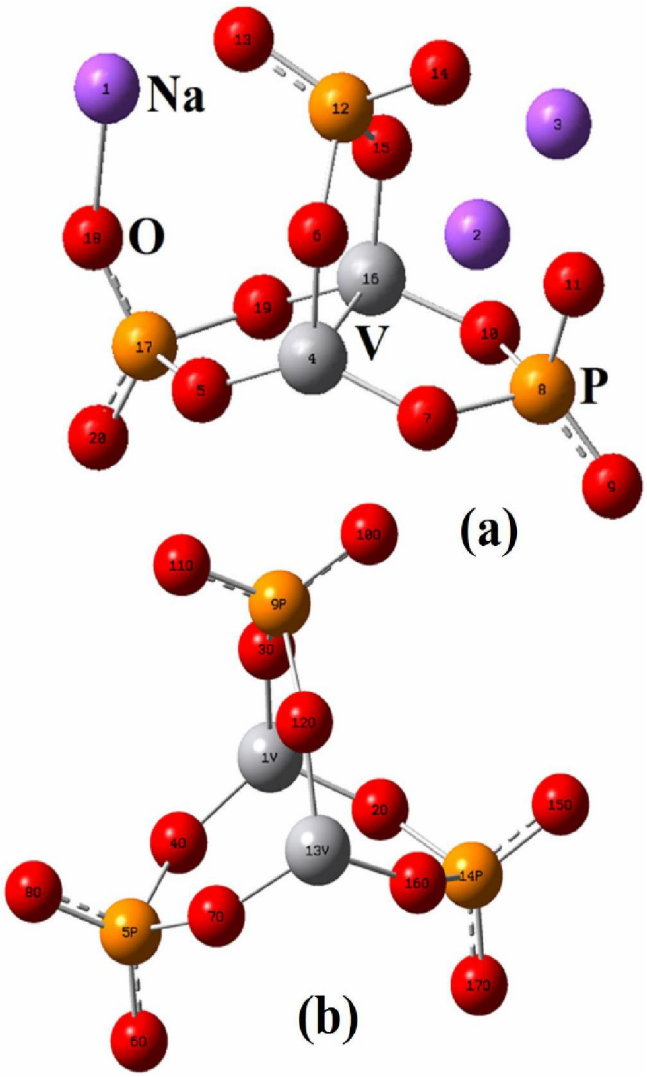

Figure 1 : The molecular structures of studied $Na_3V_2(PO_4)_3$ compound and their anion

importance to study the Mulliken and natural charges (NPA) for the Na, P, V and O atoms, the bond orders corresponding to the P-Na, V-O, P-O and Na-O bonds, which are expressed as Wiberg indexes, and the second order perturbation theory analysis to evaluate the stability of each species. Therefore, these quantities for the two species in both media were calculated with the NBO 3.1 program[34]. On the other hand, in order to understand the behaviour electrochemical at molecular level of these species used as Na-ion batteries[1,3,4,35,36] and its difference in relation to the Li-ion batteries[6,37], it is necessary to know the inter and intra-molecular interactions and their topological properties. For these reasons, these parameters were analyzed for the two species in both media with the AIM200 program by using the atoms in molecules theory (AIM)[38,39]. The molar volumes are other interesting parameters studied for the two species in both media due to its three-dimensional structures which were calculated with the Moldraw program[40]. Besides, the harmonic frequencies and the force fields expressed in Cartesian coordinates for the two molecules were evaluated in gas and aqueous solution phases by using the SQMFF methodology[13]. Here, the Molvib program was used to transform the obtained force fields to "natural" internal coordinates[41] while these latter coordinates for $Na_3[V2(PO_4)_3]$ and their $[V_2(PO_4)_3]^{3-}$ anion were defined according to molecules with similar groups[42] and they are presented in TABLES S1 and S2 (Supporting material). For both species, the complete vibrational assignments of all the normal vibration modes were performed only considering those potential energy distribution components (PEDs) ≥ 10%.

RESULTS AND DISCUSSION

Geometry

TABLE S3 summarizes the total (*E*) and relative (ΔE) energies and the dipole moment values for the $Na_3[V2(PO_4)_3]$ compound and their anion by using different method and basis sets. The results for both species and media clearly show that the DFT methods are more adequate for these systems than the HF methods while the LanL2DZ basis set is better than the CEP-4G basis set. On the other hand, the hybrid B3P86 method produces lower energy values than the B3LYP level of theory while for both species the CEP-4G basis set genera the higher energy values. In all the calculations, the anion has C_2 symmetry and the dipole moment values are practically null in gas phase while the values slight increase in aqueous solution giving imaginary values for the frequencies by using all the methods studied with exception of the B3LYP/CEP-4G method in solution, as indicated in TABLE S3. Here an important result was observed for the ion in solution by using the B3LYP/LanL2DZ method with the IEFPCM model because the optimization produces positive frequencies in this medium but in the prediction of the Raman spectrum imaginary values were obtained.

ORIGINAL ARTICLE

Thus, for the anion the better combination in gas phase is B3LYP/LanL2DZ while in solution the approximation B3LYP/CEP-4G is the adequate to study the structural and vibrational properties. On the contrary, for $Na_3[V2(PO_4)_3]$ in both media the better results are obtained by using the B3P86/LanL2DZ level of theory. It is important to clarify that when this species is optimized with C_s symmetry imaginary frequencies values were obtained while when the structures are optimized with C_1 symmetry all the frequencies values are positive. Thus, the properties for $Na_3[V2(PO_4)_3]$ were studied considering the two B3P86/LanL2DZ and B3LYP/LanL2DZ calculation levels. TABLE 1 show the calculated geometrical parameters for the $[V_2(PO_4)_3]^{3-}$ ion and $Na_3V_2(PO_4)_3$ at different levels of theory. These values were compared with those experimental reported for this species in solid phase[5] by using X-ray diffraction by means of the root mean of square deviation (RMSD) and the values were added in the corresponding Table. Experimentally, the molecule has isolated $[VO_6]$ octahedral and $[PO_4]$ tetrahedral in a three-dimensional framework where the tree Na^+ cations have different coordination modes with different oxygen environments[3]. In general, the observed bond length values follow the tendency: P-O < V-O < Na-O < P-Na< Na-Na < V-V. Theoretically, the lowest values in the distances are calculated for the anion in both media while for the two species larger distances are observed in solution as consequence of the hydration. Another important observation is that in gas phase the distance values are approximately similar in both species while these values change notably in solution, as expected. Thus, in both species the V-V distances are predicted in both media much smaller than the experimental one. Note that in the experimental structure the two P=O double bonds of the three PO_4 groups have the same values while the P-O simple bonds are slightly different from the double bonds and the six V-O bonds are equivalent among them. On the other hand, the theoretical calculations predicted for all the bonds higher values than the experimental ones and notable differences between the P=O and P-O bonds. It observation is supported because the O-P-O angles corresponding to the three PO_4 groups are forming rings. In relation to the bond angles the theoretical calculations predicted higher values than the experimental ones. The entire observed O=P=O angles have values of 108.7º while the values for the O-P-O angles linked to O-V bonds are 111.7º. The values for the O-V-O and O-V-V angles are 96.4 and 59.4º, respectively. The theoretical calculations show that for both species the values of the O=P=O and O-V-V angles decrease in solution while the internal O-P-O angles increase their values by the hydration. The different calculations predicted for both species in solution notable changes in the dihedral angles. Hence, for the ion, these angles increasing notably in solution while for $Na_3[V2(PO_4)_3]$ a decreasing is observed in this medium, as can be seen in TABLE S4.

Volume variations and solvation energy

The changes observed for the two species in the geometrical parameters in solution are evidenced by the calculated volume variations, as observed in TABLE S4. These parameters were calculated as the difference between the values in aqueous solution (V_{AS}) and the values in gas phase (V_G)[40]. The results for both species show in general volume contractions in solution but the B3LYP/LanL2DZ method predicted high volume expansions for both species in solution. Thus, the hydrations of both species are expected in aqueous solution being higher in the ion because it is a highly charged species in this medium. Consequently, the solvation energies were obtained for both species, as observed in TABLE S4. The parameters uncorrected (ΔG_u), corrected (ΔG_c), and the total non electrostatic terms (ΔG_{ne}) solvation energies due to the cavitation, dispersion and repulsion energies were calculated by means the IEFPCM/SMD model[7,42]. The solvation energy values by using all the methods show the high hydration of the anion in solution in reference to the values for the neutral species. Note that the presence of three Na^+ ions in the neutral species produces with all the used methods increasing in the molar volumes and decreasing in the solvation energy values.

Atomic charges and bond orders

The Mulliken and natural charges (NPA) for all

ORIGINAL ARTICLE

TABLE 1 : Calculated geometrical parameters for the $[V_2(PO_4)_3]^{3-}$ ion and $Na_3V_2(PO_4)_3$ at different levels of theory

Parameters	B3LYP/Lanl2DZ[a]		B3P86/Lanl2DZ[a]		Exp.[b]
	GAS	PCM	GAS	PCM	
Bond Length (Å)					
P8-O7	1.765	1.720	1.758	1.717	1.523
P8-O9	1.570	1.595	1.567	1.590	1.523
P8-O10	1.765	1.720	1.758	1.717	1.536
P8-O11	1.636	1.630	1.632	1.625	1.536
P12-O6	1.747	1.730	1.741	1.723	1.523
P12-O13	1.592	1.606	1.588	1.600	1.536
P12-O14	1.624	1.627	1.619	1.622	1.523
P12-O15	1.747	1.730	1.741	1.723	1.536
P17-O5	1.792	1.723	1.784	1.721	1.523
P17-O18	1.598	1.611	1.594	1.604	1.536
P17-O19	1.792	1.723	1.784	1.721	1.523
P17-O20	1.570	1.598	1.567	1.593	1.536
V4-O5	1.739	1.809	1.729	1.793	1.969
V4-O6	1.826	1.830	1.813	1.817	1.969
V4-O7	1.779	1.828	1.769	1.812	1.969
V4-V16	2.387	2.614	2.361	2.473	4.484
V16-O10	1.779	1.828	1.769	1.812	1.969
V16-O15	1.826	1.830	1.813	1.817	1.969
V16-O19	1.739	1.809	1.729	1.793	1.969
Na1-O13	2.233	2.268	2.229	2.265	2.505
Na1-O18	2.155	2.230	2.153	2.228	2.505
Na2-O11	2.275	2.337	2.270	2.341	2.505
Na3-O11	2.275	2.337	2.270	2.341	2.505
RMSD	0.100	0.131	0.146	0.164	
Bond angle (degrees)					
O7-P8-O10	92.7	96.6	92.8	95.8	111.7
O9-P8-O11	123.8	119.1	123.8	119.4	108.7
O7-P8-O11	101.3	106.4	101.3	106.4	106.1
O10-P8-O11	101.3	106.4	101.3	106.4	106.1
O6-P12-O15	96.6	100.6	96.6	99.2	111.7
O13-P12-O14	125.5	120.3	125.4	120.5	108.7
O13-P12-O6	111.5	111.1	111.5	111.5	106.1
O13-P12-O15	111.5	111.1	111.5	111.5	106.1
O5-P17-O19	88.4	96.0	88.5	94.4	111.7
O18-P17-O20	126.3	119.0	126.3	119.5	108.7
O5-P17-O18	104.2	108.4	104.2	108.7	106.1
O19-P17-O18	104.2	108.4	104.2	108.7	106.1
O5-V4-O6	117.2	111.7	117.5	111.4	96.4
O5-V4-O7	138.6	142.0	138.2	142.0	96.4
O5-V4-V16	91.8	89.2	92.1	90.8	59.4
O7-V4-V16	92.7	89.3	93.0	91.1	59.4
O15-V16-O10	103.3	106.1	103.4	106.3	96.4

ORIGINAL ARTICLE

Parameters	B3LYP/Lanl2DZ[a]		B3P86/Lanl2DZ[a]		Exp.[b]
	GAS	PCM	GAS	PCM	
Bond Length (Å)					
O15-V16-O19	117.2	111.7	117.4	111.4	96.4
O10-V16-O19	138.7	142.0	138.2	142.0	96.4
O10-V16-V4	92.6	89.3	93.0	91.1	59.4
O19-V16-V4	91.8	89.2	92.1	90.8	59.4
O13-Na1-O18	122.8	125.1	122.9	123.2	160.5
Na2-O11-Na3	92.6	89.0	93.1	89.0	85.4
Na2-O14-Na3	87.1	87.1	87.4	87.3	84.2
RMSD	4.6	4.3	4.6	4.4	
Dihedral angles(degrees)					
O9-P8-O7-V4	-143.6	-148.9	-143.6	-148.9	-146.92
O9-P8-O10-V16	143.6	148.9	143.5	148.9	94.52
O20-P17-O5-V4	136.4	132.7	136.1	131.2	94.45
O20-P17-O19-V16	-136.4	-132.7	-136.1	-131.2	-146.92
O20-P17-O18-Na1	179.9	179.9	-179.9	180.0	168.39
Na1-O13-P12-O14	179.9	-179.9	-179.9	-180.0	173.32
P8-O11-Na2-O14	-116.8	-108.0	-117.0	-108.7	-98.03
P8-O11-Na3-O14	116.9	108.0	117.0	108.7	114.42
RMSD	8.7	45.0	62.6	45.0	

[a]This work; [b]Experimental for $Na_3V_2(PO_4)_3$ from Ref[5].

the Na, P, V and O atoms of the two species in both media were calculated with the NBO 3.1 program[34] and they can be seen in TABLE S5. The results show notable differences between both charges and a strong dependence of the charges with the size of the basis set. Thus, the values of both charges for the V atoms of the anion are similar among them only in gas phase while the values completely change in solution due to the different methods used. In the anion, all the charges are equivalent as consequence of the symmetry while in the neutral species the existence of three Na^+ ions in the structure generates differences in the values of both charges for all the atoms due to the different environmental. Thus, an increase in the Mulliken charges corresponding to the V atoms in gas phase is observed while these charges decrease in solution, in accordance with the Na^+ cations whose charges diminish in this medium. Here, the proximity of the Na^+ ions at the O11, O14 and O15 atoms increase the charge values on these atoms (see Figure 1). Another very important observation for this species in solution is the strong increasing in the charges on the P and O atoms with the hydration due to the H bonds formation. For the three Na^+ ions both charges increase confirming the solvation of these species in solution. Note that both charges in solution on the P12 atom are slightly lower than the P8 and P17 ones. Figure S1 show the calculated electrostatic potential surfaces for the ion where the strong red coloration on the surface reveals clearly the potential nucleophilic sites because the species is an anion. On the contrary, the calculated electrostatic potential surfaces for $Na_3[V2(PO_4)_3]$ present blue color on the Na^+ ions, as observed in Figure S2 because this color is related with potential electrophilic regions. These calculations for this species in both media show clearly the Na2-Na3, P12←Na2 and P12←Na3 bonds.

The bond orders corresponding to the different bonds of both species were studied in both media and the values expressed as Wiberg indexes can be seen from TABLE S6 to S10. The bond order totals by atom for both species in the two media studied are presented in TABLE S6. In this study, the results for the ion show also a strong dependence of the bond orders with the size of the basis set. Thus, dif-

ferent coordination modes are calculated for the V atoms in both species, for instance, for the neutral species in solution the bond orders for all the atoms decrease in solution, as it is expected due to the solvation. TABLE S7 show the bond orders index matrix for the atoms from 1 to 9 corresponding to the ion in gas phase at B3LYP/LanL2DZ level of theory and, in solution by using the B3LYP/CEP-4G method. TABLE S8 show the bond orders index matrix for the atoms from 10 to 17 corresponding to the ion in both media at the same levels of theory mentioned. For the ion, the values shows in both media higher bond orders for the O atoms linked to the V atoms that clearly increase its values in solution due to the hydration. The coordination for the two V atoms of 3.501 in gas phase increase at 4.725 in solution evidenced by the solvation of the anion in aqueous solution. For all the atoms of $Na_3V_2(PO_4)_3$ the bond order totals by atom increasing slightly with the hydration showing the two V atoms of this species in both media a five coordination, as observed in TABLES S9 and S10. Thus, in the anion the V has valence (III) while in the neutral species the valence observed is (V).

In this work, for both species the calculated natural hybrids (NHOs) on V-O positions, polarisation coefficients (CV, CO) of each hybrid in the corresponding NBO and calculated σV-O and lone pairs (LP*V) bond orbital occupancies were also reported in TABLES S11 and S12. For the ion, the results in both media show that in all the σV-O orbitals the higher polarization coefficients are observed for the O atoms, as expected because these atoms have higher electronegativities while in solution increase the polarization coefficients for the V atoms and the occupation in some σV-O orbitals because increase the p character of the O atom and the d character of the V atoms as consequence of the H bonds formation on the O atoms. Additionally, new σ*V-O orbitals appear in solution by the hydration, as indicated in TABLE S11. On the contrary, for the neutral species from the twelve σV-O and σ*V-O orbitals observed in gas phase eight are observed in solution increasing their occupations and the polarization coefficients for the V atoms while the number of LP*V orbitals increase from four in gas phase to eight in aqueous solution. These different studies show clearly that the hydration take place in both species.

NBO and AIM studies

The evaluation of the stabilities of $[V_2(PO_4)_3]^{3-}$ and $Na_3V_2(PO_4)_3$ is important to understand the behaviour electrochemical of these species in relation to its use as Na-ion batteries[1,3,4,35,36] and, moreover to know the differences with the Li-ion batteries[6,37]. From this point of view, the two species were studied by using NBO calculations[34] and AIM analysis[38,39]. TABLE S13 show the main delocalization energies for the $[V_2(PO_4)_3]^{3-}$ ion in both media at different levels of theory while the same properties for $Na_3V_2(PO_4)_3$ at B3LYP/LanL2DZ levels of theory are presented in TABLE S14. In both media, for the ion are observed the $\Delta ET_{\sigma\rightarrow\sigma^*}$, $\Delta ET_{LP\rightarrow\sigma^*}$ and $\Delta ET_{LP\rightarrow LP^*}$ charge transfers while in solution the additional $\Delta ET_{\sigma^*\rightarrow\sigma^*}$ charge transfers support the high stability of this species in solution because the ΔE_{Total} of 2162.9 kJ/mol in gas phase increase at 19919.6 kJ/mol in solution. For the neutral species are observed a high number of contributions of the stabilization energies to the total energy, thus, the $\Delta ET_{\sigma\rightarrow\sigma^*}$, $\Delta ET_{LP\rightarrow\sigma^*}$, $\Delta ET_{\sigma^*\rightarrow\sigma^*}$, $\Delta ET_{\sigma^*\rightarrow LP^*}$, $\Delta ET_{LP\rightarrow LP^*}$ and $\Delta ET_{LP^*\rightarrow LP^*}$ charge transfers are observed in both media while in solution the supplementary $\Delta ET_{\sigma\rightarrow LP^*}$ charge transfers reveals the high stability of $Na_3V_2(PO_4)_3$ in solution due to the H bonds because the ΔE_{Total} of 23611.3 kJ/mol in gas phase increase at 37150.3 kJ/mol in solution. The high values of the two $\Delta ET_{\sigma^*\rightarrow\sigma^*}$ and $\Delta ET_{\sigma^*\rightarrow LP^*}$ charge transfers of 18935.7 and 11032.6 kJ/mol, respectively suggest that the presence of the three Na^+ ions clearly increase the stability of the neutral species because has a higher volume (TABLE S4).

The different interactions for both species in gas phase and in solution were also studied by using the AIM program by means of the topological properties calculations[39,43]. TABLE S15 show the analysis of the bond critical points (BCP) for the $[V_2(PO_4)_3]^{3-}$ ion at different levels of theory in gas and aqueous solution phases while in TABLES S16 and S17 are presented the results of this investigation for $Na_3[V_2(PO_4)_3]$. Thus, the parameters such

ORIGINAL ARTICLE

as, the electron density distribution, $\rho(r)$ in the bond critical points (BCPs), the values of the Laplacian, $\nabla^2\rho(r)$, the eigenvalues $(\lambda1, \lambda2, \lambda3)$ of the Hessian matrix at these points matrix and, the $\lambda1/\lambda3$ ratio are calculated in those Tables. This latter ratio allows the description of the character of interaction between atoms. Thus, when $\lambda1/\lambda3 > 1$ and $\nabla^2\rho(r) < 0$ the interaction is typical of covalent bonds (called shared interaction) with high values of $\rho(r)$ and $\nabla^2\rho(r)$ while when $\lambda1/\lambda3 < 1$ and $\nabla^2\rho(r) > 0$ the interaction is called closed-shell interaction and is typical of ionic, highly polar covalent and hydrogen bonds as well as of the van-der-Waals and specific intermolecular interactions[43]. For the anion in both media we observed six O—O interactions with similar properties in the BCPs ($\rho(r)$= 0.0848, $\nabla^2\rho(r)$= -0.2162 and $\lambda1/\lambda3 > 1$) and one V—V interaction with values in the BCPs of $\rho(r)$ between 0.0145 and 0.0107, of $\nabla^2\rho(r)$ between 0.0296 and 0.0174 and $\lambda1/\lambda3 < 1$. The first O—O contacts, correspond to the O atoms belonging to the three PO_4 groups, indicate that they are shared interactions and are typical of covalent bonds, as observed in Figure S3. The characteristic of the other V—V contacts are those closed-shell interactions typical of ionic bonds. The calculations for the anion show that $\rho(r)$ increase in solution while $\nabla^2\rho(r)$ and the $\lambda1/\lambda3$ ratio decrease as consequence of the hydration. The presence of the V—V ionic interactions justifies the ionic properties of this anion in both media. Table S16 show the analysis of the BCPs corresponding to the O-V bonds of $Na_3[V_2(PO_4)_3]$ in both media at different levels of theory. In this case the calculated properties ($\rho(r)$ = 0.1294, $\nabla^2\rho(r)$ =0.6384 and $\lambda1/\lambda3$= 0.2045) suggest interactions ionic, as expected because the O atom has higher electronegativity than the V atom. TABLE S17 show the analysis of the BCPs for the O—O and V—V interactions corresponding to $Na_3V_2(PO_4)_3$ at different levels of theory. From the sixteen O—O interactions observed in both media for this species fourteen are typical of covalent bonds while the two remaining O11—O14 and O13—O18 connections have properties typical of hydrogen bonds ($\rho(r) \leq 0.07$ a. u., $|\lambda1|/\lambda3 < 1$ and $\nabla^2\rho(r)$ = 0.10-0.30 a. u.)[9,10]. In this neutral species, the V—V interactions are also ionic, as those observed for the anion. For this species in solution, the calculations show that in general $\rho(r)$ decrease while $\nabla^2\rho(r)$ and the $\lambda1/\lambda3$ ratio increase as consequence of the hydration, a result different from those observed for the anion. Another significant result for this species is that in gas phase is only observed the covalent O6—O15 interaction while in aqueous solution the only observed is the covalent O9—O10 interaction. The first interaction is justified because the O6-O15 distance in gas phase is 2.610 Å while in solution increase at 2.663 Å while the second interaction is attributed to the O9-O10 distance between both atoms because in gas phase is of 2.832 Å the which decrease in solution at 2.762 Å. These results shows: (i) the high stability of $Na_3[V_2(PO_4)_3]$ and their anion attributed to the presence of covalent, ionic and of H bonds interactions in the compound and, to the covalent and ionic interactions in the anion, (ii) the ionic nature of $Na_3[V_2(PO_4)_3]$ and their anion in conformity with the experimental structure determinate by X-ray-diffraction[5].

HOMO-LUMO study

For $Na_3[V_2(PO_4)_3]$ and their anion we have also calculated the HOMO and LUMO frontiers orbitals and energy band gaps[44] to predict their behaviors and reactivities in gas and aqueous solution phases. The maps of electrostatic potentials have showed nucleophiles sites on the molecular surfaces of the anion and electrophiles sites on the Na^+ ions of $Na_3[V_2(PO_4)_3]$ (Figures. S1 and S2). The knowledge of these properties is important to understand the electrochemical properties of the two species in both media. TABLE 18 show the calculated HOMO and LUMO orbitals and energy band gaps for both species at different levels of theory. Taking into account the C_2 symmetry for the anion, the HOMO and LUMO orbitals were calculated with A_2'' and E' symmetries, respectively while both orbitals are mainly localized on the pz and d orbitals of the V atoms in the anion and, on the d orbitals of the V atoms for the neutral species. Comparing first the energy band gaps for each species, we observed that in solution the ion is less reactive, a result different from that expected because it is an ion and, for this reason, it should have high affinity by this solvent. Probably,

the CEP-4G basis set used for the calculations in solution justifies this resulted. On the other hand, the neutral species is clearly more reactive in both media. Comparing both species, we observed that the presence of the three Na^+ ions in the compound produces the reduction of the HOMO-LUMO gaps in both media indicating that this species has a higher reactivity than the anion while the low values of the HOMOs for $Na_3[V_2(PO_4)_3]$ in the two media predicted the higher stabilities for this species. An interesting result is that both frontiers orbitals for $Na_3[V_2(PO_4)_3]$ and their anion have the same numbering, as observed in TABLE S18, thus, the 70 and 71 orbitals correspond to HOMO and LUMO, respectively. The existence of three Na atoms as cations justifies the same numbering for these orbitals in the neutral species.

Vibrational analysis

The anion structures with both methods used are optimized with C_2 symmetry and, for this reason; it has 45 active vibrational normal modes in both infrared and Raman spectra. As explained in the Section 3.1, for the anion in gas phase the vibrational properties was performed by using the combination B3LYP/LanL2DZ while in solution the approximation B3LYP/CEP-4G is the adequate for this study. For $Na_3[V_2(PO_4)_3]$, the analysis in both media was performed by using the B3LYP/LanL2DZ and B3P86/LanL2DZ levels of theory. This species has C_1 symmetry and 54 vibrational normal modes active in both vibrational spectra Figure 2 show the available experimental infrared taken from Ref.[6] compared with those calculated for the anion and the neutral species while in Figure 3 the predicted Raman spectrum for $Na_3[V_2(PO_4)_3]$ by using the B3LYP/LanL2DZ method is observed. A comparison between the theoretical infrared spectra for $Na_3[V_2(PO_4)_3]$ and their anion in gas phase by using B3LYP/LanL2DZ level of theory is presented in Figure S4. The assignments of the observed bands in the infrared (IR) spectra of $Na_3[V_2(PO_4)_3]$ to the normal vibration modes were performed taking into account the PED contributions obtained by SQM calculations and by comparison with related molecules[6,26,42,45]. TABLE 3 show the experimental and calculated wavenumbers and the corresponding assignments for the $[V_2(PO_4)_3]^{3-}$ ion and $Na_3V_2(PO_4)_3$ at different levels of theory. TABLES S19 and S20 shows the calculated frequencies for the $[V_2(PO_4)_3]^{3-}$

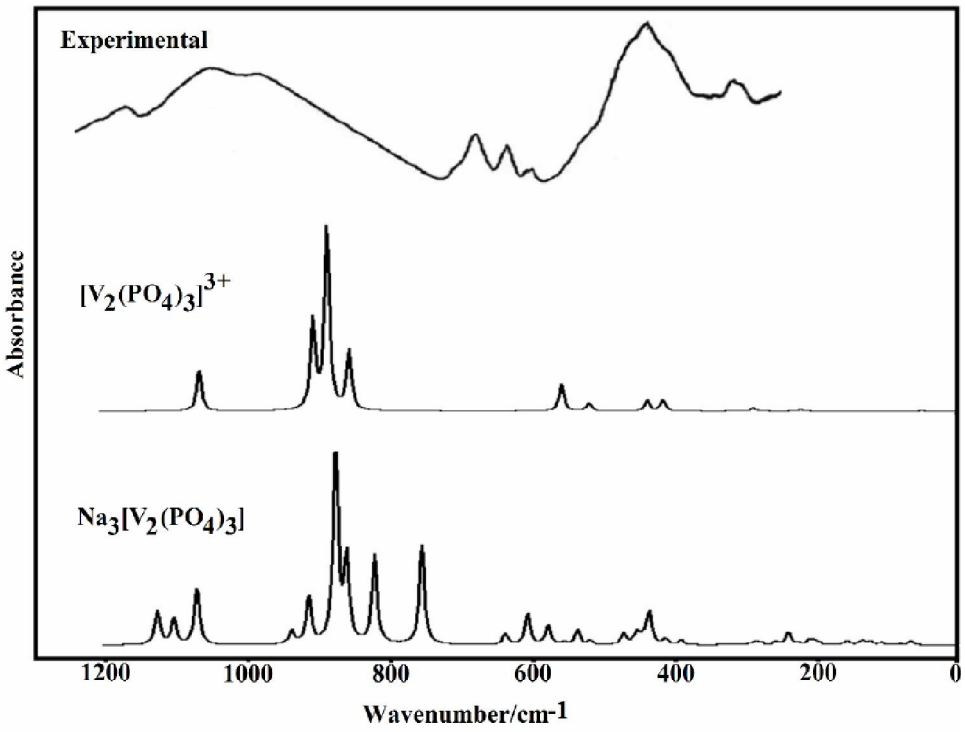

Figure 2 : Comparison between the experimental available infrared spectra and the corresponding to the $Na_3V_2(PO_4)_3$ compound and their anion

ORIGINAL ARTICLE

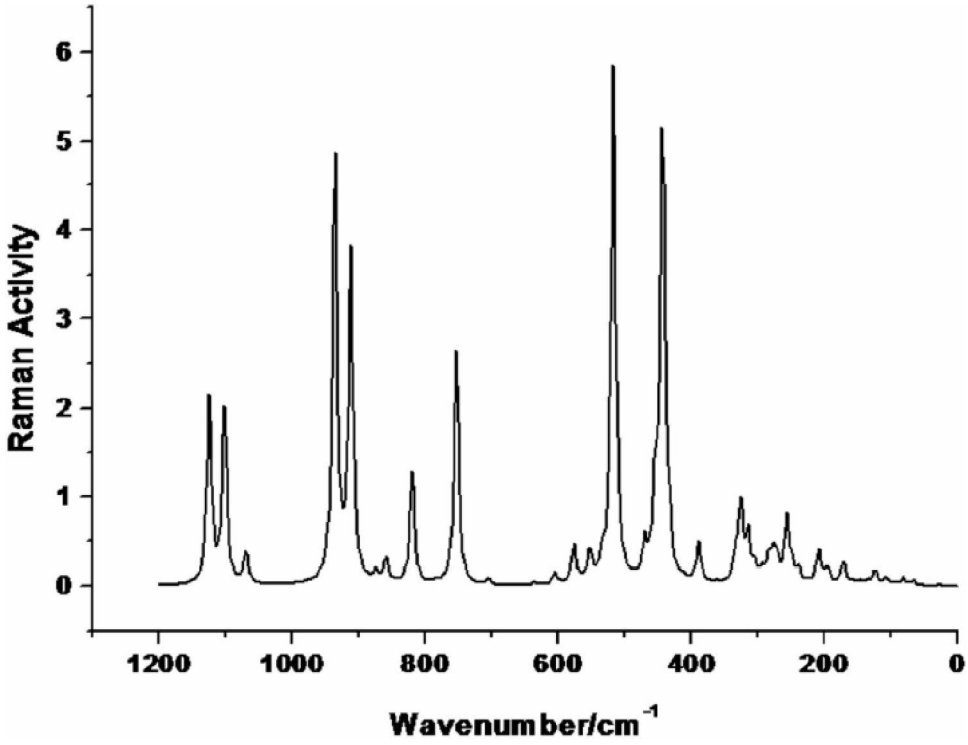

Figure 3 : Predicted raman spectrum for $Na_3V_2(PO_4)_3$ at the B3LYP/Lanl2dz level of theory

ion in gas and aqueous solution by using B3LYP/ Lanl2DZ and B3P86/CEP-4G levels, respectively and, the potential energy distribution based on these two approximations levels. TABLES S21 and S22 shows the calculated frequencies for $Na_3[V_2(PO_4)_3]$ in gas and aqueous solution and, the potential energy distribution based on the B3LYP/Lanl2DZ and B3P86/ Lanl2DZ levels. Figure S5 show a comparison between the experimental infrared spectra for $Na_3[V_2(PO_4)_3]$ with the theoretical by using B3LYP/ LanL2DZ and B3P86/ Lanl2DZ levels of theory. Note that both spectra demonstrate a good agreement with the experimental spectrum, as observed in Figures. 2 and S5. The calculated harmonic force field for the compound studied can be obtained upon request. A discussion of the assignments for each species in presented below.

PO4 groups

The P=O antisymmetric and symmetric stretchings in tetrahedral phosphate groups[42,45] are expected between 1150 and 816 cm^{-1}. In $Na_3[V_2(PO_4)_3]$ the three antisymmetric modes in both media are calculated at different wavenumbers because they have different environmental, thus, these modes are assigned to the IR bands between 1180 and 1045 cm^{-1}. The corresponding symmetric stretchings are predicted between 912 and 826 cm^{-1} and, for this reason, they are assigned in this region, as observed in TABLE 3. Note that for the anion in gas phase these modes are calculated in the same region that for $Na_3[V_2(PO_4)_3]$ but, in solution they are predicted at lower wavenumbers, as can be seen in TABLE 3. The PO_2 antisymmetric and symmetric stretching modes are predicted in different regions in gas and aqueous solution phases, as expected because they correspond to the simple bonds. Thus, in gas phase both modes are associated with the IR bands between 589 and 435 cm^{-1} while in solution are calculated between 791 and 553 cm^{-1}. This way, both strechings modes are assigned to the shoulder and bands observed between 791 and 435 cm^{-1}. In the anion, these modes are associated with the bands between 530 and 390 cm^{-1}, as predicted by the calculations in the two media. Notable differences in gas phase and in solution are observed in the regions calculated for the six expected O=P=O and O-P-O bending modes because they are predicted strongly mixed among them, as observed in TABLE 3. Thus, in gas phase those modes are calculated by SQM calculations at 439, 318 and 299 cm^{-1} while in

ORIGINAL ARTICLE

TABLE 2 : Observed and calculated wavenumbers (cm^{-1}) and assignments for the $[V_2(PO_4)_3]^{3-}$ ion and $Na_3V_2(PO_4)_3$ at different levels of theory

IR[b]	$[V_2(PO_4)_3]^{3-}$ ion[a]				$Na_3V_2(PO_4)_3$[a]			
	GAS PHASE		PCM		GAS PHASE		PCM	
	SQM[c]	Assignments[a]	SQM[d]	Assignments[a]	SQM[e]	Assignments[a]	SQM[f]	Assignments[a]
1180 m	1016	ν_a P=O_2ip			1079	ν_aP=O_2(P17)	1025	ν_aP=O_2(P17)
1125 sh	1016	ν_aP=O_2(P9)			1057	ν_aP=O_2(P8)	1020	ν_aP=O_2(P8)
1045 s	1010	ν_a P=O_2op			1025	ν_aP=O_2(P12)	1007	ν_aP=O_2(P12)
975 sh	899	ν_sP=O_2 ip			901	ν_sP=O_2(P17)	912	ν_sP=O_2(P17)
	868	ν_sP=O_2 op			878	ν_sV-O	879	ν_sP=O_2(P8)
	868	ν_sP=O_2(P9)						
	849	ν_aV-O_3op					855	ν_sP=O_2(P12)
840 sh	848	ν_aV-O_2op			842	ν_sP=O_2(P12)		
	825	ν_sV-O_3ip	813	ν_a P=O_2op	826	ν_sP=O_2(P8)		
			813	ν_a P=O_2ip				
	819	ν_sV-O_3op	812	ν_aP=O_2(P9)			818	ν_sV-O
					788	ν_sV-O	791	ν_sP-O_2(P8)
			759	ν_aV-O_3op				
			759	ν_aV-O_2op	758	ν_aV-O		
	715	ν_aV-O_2ip	748	ν_sV-O_3ip	726	ν_sV-O	742	ν_sV-O
	714	ν_aV-O_3ip	703	ν_sV-O_3op				
			686	ν_sP=O_2(P9)				
			685	ν_sP=O_2 op				
670 sh			680	ν_sP=O_2 ip	682	ν_aV-O	685	ν_aV-O
			648	ν_aV-O_2ip			659	ν_aV-O
			647	ν_aV-O_3ip				
625 m							625	ν_aP-O_2(P12)
					617	ν_aV-O	616	ν_aV-O
					589	ν_aP-O_2(P12)	593	ν_aP-O_2(P8)
575 m							579	ν_sP-O_2(P17)
550 sh					557	ν_sP-O_2(P12)	554	ν_sP-O_2(P12)
	542	wagP=O_2ip			534	ν_sP-O_2(P8)	553	ν_aP-O_2(P17)
530 sh	501	ν_sP-O_2(P9)			516	ν_aP-O_2(P8)		
	501	ν_sP-O_2op			501	ν_sP-O_2(P17)	504	ν_sV-O
480 sh	486	ν_aP-O_2(P9)						
	484	ν_aP-O_2op	481	wagP=O_2ip				
470 sh	479	δ_sP=O_2	465	ν_sP-O_2(P9)	470	δO6P12O15	471	δO14P12O13
			461	ν_sP-O_2op				
440 sh					439	δO18P17O20	440	δO5P17O19 δO18P17O20
					435	ν_aP-O_2(P17)	435	δO7P8O10
	437	δ_sPOV			434	δO7P8O10		
	409	δP-O_2(P9)						
400 sh	408	δ_aP-O_2	418	ν_sP-O_2ip	412	? wP=O_2(P12)		
	397	τwP=O_2op	393	ν_aP-O_2(P9) ν_aP-O_2op			402	τwP=O_2(P12)
	396	τwP=O_2(P9)	390	ν_aP-O_2op	382	ν_aNa-O11		

ORIGINAL ARTICLE

IR[b]	$[V_2(PO_4)_3]^{3-}$ ion[a]				$Na_3V_2(PO_4)_3$[a]			
	GAS PHASE		PCM		GAS PHASE		PCM	
	SQM[c]	Assignments[a]	SQM[d]	Assignments[a]	SQM[e]	Assignments[a]	SQM[f]	Assignments[a]
375 sh					377	τwP=O_2(P8)	370	τwP=O_2(P8)
							366	wagP=O_2(P8), ρP=O_2(P12)
355 vs	355	τwP=O_2ip			355	$\delta_a VO_2$		
340 sh					354	τwP=O_2(P17)	349	$\delta_a VO_2$
	339	δVO_2ip					346	τwP=O_2(P17)
	339	δVO_3op						
			316	δVO_2ip	322	δVO_2	325	wagP=O_2(P17)
			308	δVO_3op	318	δO14P12O13		
	305	δVO_3op	302	τwP=O_2op	304	νV4-V16	307	δO6P12O15
			299	δ_aP=O_2	299	δO9P8O11	299	wagP=O_2(P12)
280 sh	283	δP=O_2(P9)	291	δ_sPOV	292	δPOV(P12), wagP=O_2(P12)	295	δO9P8O11
	282	δ_aP=O_2	287	τwP=O_2(P9)	281	ρP=O_2(P17)	285	δPOV(P12)
270 sh	274	ν_sP-O_2ip					279	νV4-V16
	273	wagP=O_2op					276	ρP=O_2(P8)
	272	wagP=O_2(P9)						
	269	ρP=O_2ip	260	δVO_3op	269	ν_sNa1-O		
			259	δP=O_2(P9)	267	ρP=O_2(P12)	256	ν_sNa1-O
			245	δ_aP-O_2 ρP=O_2op	249	δO5P17O19		
240 m			243	τwPOV(P9)	241	$\delta_a VO_2$	242	δVO_2
225 sh			230	wagP=O_2op	230	ν_sP12-Na	228	ν_aNa1-O
			228	wagP=O_2(P9)			220	ν_sP12-Na
	214	ν_aP-O_2op			218	wagP=O_2(P8)	208	ρP=O_2(P17) τwP17O18
190 sh			198	ρP=O_2ip δ_sP=O_2	202	ν_sNa-O11	203	ρP=O_2(P17)
			197	τwP=O_2ip	195	ν_aP12-Na	198	ν_sNa-O11
					187	ν_aNa1-O	179	τwP8-O11 ν_sNa-O11
175 sh			171	δP-O_2(P9)	176	δPOV	178	δPOV
	162	νV1-V13	168	δ_aP-O_2			171	δ_sV-O_3
	161	δVO_2ip						
	161	δVO_3ip			162	δ_sV-O_3	161	ν_aNa-O11
	155	ρP=O_2(P9)						
	154	δPOV(P9)			154	ρP=O_2(P8)	150	$\delta_a VO_3$
			145	δPOV(P9)	145	τwP17-O20 τwP17O18	142	τwP17-O20 τwP17O18
			144	δ_aPOV				
					129	δNa2O11Na3	127	δNa2O11Na3
			116	δVO_3ip	122	$\delta_a VO_3$		
			114	δVO_2ip				
			107	νV1-V13		τwP8-O11[#]		
			102	ρP=O_2(P9)				τwP17O18[#]

IR[b]	$[V_2(PO_4)_3]^{3-}$ ion[a]				$Na_3V_2(PO_4)_3$[a]			
	GAS PHASE		PCM		GAS PHASE		PCM	
	SQM[c]	Assignments[a]	SQM[d]	Assignments[a]	SQM[e]	Assignments[a]	SQM[f]	Assignments[a]
95	ρP=O_2op	101	ρP=O_2op	98	τwP12-O13	96	τwP8-O11	
95	δ_aPOV	85	δ_sPOV	81	τwP17-O20	83	τwP17-O20	
70	τwP=O_2op			76	τwP8-O11	82	τwP12-O13	
61	τwPOV(P9)			66	δP17O18Na1	72	τwP17O18	
46	τwP=O_2(P9)			63	τwP17O18	62	δP17O18Na1	
46	τwPOV	54	τwP=O_2op	42	ρONa_2	40	ρONa_2, ν_aP12-Na	
		25	τwPOV					
		20	τwP=O_2(P9)					

[a]This work; [b]From Ref.[6]; [c]From SQM/B3LYP/LanL2DZ calculations in gas phase; [d]From SQM/B3P86/CEP-4G calculations in aqueous solution; [e]From SQM/B3LYP/LanL2DZ calculations in gas phase; [f]From SQM/B3P86/LanL2DZ calculations in aqueous solution; [#]Assigned by GaussView program[30]

TABLE 3 : Comparison of scaled internal force constants for the $[V_2(PO_4)_3]^{3-}$ ion and the $Na_3V_2(PO_4)_3$ compound at different levels of theory

Force constants	$[V_2(PO_4)_3]^{3-}$ ion[a]				$Na_3V_2(PO_4)_3$[a]			
	B3LYP/LanL2DZ		B3LYP/CEP-4G		B3LYP/LanL2DZ		B3P86/LanL2DZ	
	GAS	PCM	GAS	PCM	GAS	PCM	GAS	PCM
f(νP=O)	5.42	5.28	3.56	3.29	5.58	5.25	5.79	5.46
f(νP-O)	2.40	3.14	1.46	1.74	2.53	3.46	2.69	3.26
f(νV-O)	7.47	5.41	8.32	6.95	3.89	3.23	4.05	3.28
f(νV-V)	0.80	0.51	0.64	1.24	1.47	1.95	1.58	1.16
f(νNa-O)					0.61	0.47	0.62	0.49
f(νP-Na)					0.48	0.39	0.49	0.42
f(δO=P=O)	1.38	1.21	0.79	0.71	1.48	1.46	1.49	1.64
f(δO-P-O)	2.04	1.56	1.30	2.13	2.09	2.14	2.07	1.82
f(δO-V-O)	1.25	0.89	1.34	1.82	1.28	1.68	1.26	1.36
f(δP-O-V)	0.68	0.62	0.62	1.00	1.73	3.36	1.79	1.70
f(δP-O-Na)					0.34	0.61	0.34	0.34
f(δNa-O-Na)					0.70	1.05	0.69	0.88

Units are mdyn Å^{-1} for stretching and mdyn Å rad^{-2} for angle deformations; [a]This work

solution at 471, 440 and 295 cm^{-1}, for these reasons, they were assigned in those regions, as indicated in TABLE 3. Despite the three PO_4 groups for the anion are equivalent those bending modes are also predicted by SQM calculations in different regions in both media. Thus, in gas phase they are calculated at 479, 283 and 282 cm^{-1} while in solution at 299, 259 an 198 cm^{-1}. The differences observed are attributed to the CEP-4G basis set because it is not very good as observed in the energy values (TABLE S3). The wagging, rocking and twisting modes for the three PO_2 groups (double bond) are clearly predicted in gas phase between 412 and 154 cm^{-1} while in solution between 402 and 203 cm^{-1}. Thus, these modes can be assigned to the shoulder and bands in those regions. For the anion in solution these modes are predicted in the lower wavenumbers region, as calculated by the two different theoretical methods.

O-V-O groups

The six expected V-O stretchings modes for $Na_3[V_2(PO_4)_3]$ are predicted with PED contributions between 43 and 68% in gas phase and between 12 and 46% in aqueous solution, as observed in TABLES S21 and S22, respectively. On the other hand, the symmetric stretchings are calculated in the

ORIGINAL ARTICLE

IR and Raman spectra in gas phase with higher intensities than the antisymmetrical modes. Thus, in gas phase those modes are calculated at 878, 788, 758, 726, 682 and, 617 cm^{-1} while in solution they are calculated at 818, 742, 685, 659, 616 and 504 cm^{-1}. Hence, these stretchings modes are assigned as can be seen in TABLES 3. For the anion in both phases, the two methods predicted the six stretchings modes between 849 and 647 cm^{-1} and with higher intensities the antisymmetrical modes out-of-phase, as observed in TABLES 19 and 20. Note that the influence of the Na^+ ions on the V-O bonds of $Na_3[V_2(PO_4)_3]$ are the shifting of the bands related to these bonds toward lower wavenumbers. For the two species, the O-V-O bending modes are predicted in the 355-122 cm^{-1} region, consequently they were assigned to the shoulders and bands observed in this region. Taking into account that the two VO_3 groups in both species are linked by means of connections V-V, as observed in Figure 1, we observed that another effect of the Na^+ ions on those groups are the shifting of the V-V stretchings modes towards higher wavenumbers, therefore, in $Na_3[V_2(PO_4)_3]$, these the V-V stretchings are calculated at 304 cm^{-1} in gas phase and at 279 cm^{-1} in aqueous solution while, in the anion, they are predicted at 162 and 107 cm^{-1} in gas and solution phases, respectively. For this reason, the shoulder at 340 and 270 cm^{-1} were assigned to these vibration modes.

Modes related to Na^+ ions

As observed in Figure 1, the optimized $Na_3[V_2(PO_4)_3]$ structure presented clearly a Na1-O18 bond while the two $Na2^+$ and $Na3^+$ ions apparently are not linked to other atoms, however, in the map of electrostatic potential surface (see Figure S2) the figure show the bonds Na1-O13, P12-Na2, P12-Na3 and Na2-Na3 bonds. The latter bond was not definite during the vibrational analysis by means of the internal normal coordinates but, the remaining bonds were confirmed by this analysis. Thus, for $Na_3[V_2(PO_4)_3]$ the vibration normal modes related with these bonds are predicted in the lower wavenumbers region (382-40 cm^{-1}). Accordingly, the Na1-O symmetric stretching modes are predicted by SQM calculations in gas phase at 269 and 202 cm^{-1} with a PED contribution of between 25 and 28 % and, in solution, these modes are calculated shifted at 256 and 198 cm^{-1} for this reason, they are without difficulty assigned to the shoulders at 270 and 190 cm^{-1}. The Na1-O antisymmetric stretching modes are assigned to the shoulders at 400 and 190 cm^{-1}, as predicted by the calculations. The two expected P12-Na stretching modes are predicted in gas phase at 230 and 195 cm^{-1} while in solution are calculated with 23 and 24% of PED contribution at 220 and 40 cm^{-1}, hence, these were only assigned to the shoulders at 225 and 190 cm^{-1}. The Na-O-Na bending modes were predicted by calculations in the same regions, as well in gas phase as in solution, at 129/127 and 66/62 cm^{-1}, in consequences these modes together with the $O\text{-}Na_2$ rocking modes could not be assigned due to their low frequencies.

Skeletal modes

In $Na_3[V_2(PO_4)_3]$ and their anion, the skeletal bending and torsion modes appears strongly coupled among them as can be seen from TABLES S19 to S22. Taking into account the positions predicted by the calculations for $Na_3[V_2(PO_4)_3]$, the expected P-O-V bending modes were associated with the two shoulders at 280 and 175 cm^{-1} while for the anion these modes are predicted in different regions for the which one of these modes was only assigned, as can be seen in TABLE 3.

FORCE CONSTANTS

Taking in consideration the results obtained by the above studies, the force constants were also calculated for both species in the two media in order to known the nature and forces of the different P=O, P-O, V-O, V-V, P-Na and Na-O bonds and also, the constants for the more important angle deformations. These constants were calculated using the Molvib program[41] and the force fields for both species. TABLE S3 show a comparison of the scaled internal force constants for the $[V_2(PO_4)_3]^{3-}$ ion and the $Na_3V_2(PO_4)_3$ compound at different levels of theory and in the two studied media. In general, it is observed that all the force constants values are strongly dependent of the size of the basis sets and, a de-

creasing in their values in solution are observed. The following results are obtained for the anion and $Na_3V_2(PO_4)_3$, the *f(νV-O)* force constants are higher than the *f(νP=O)* force constants with the two methods of calculations and in the two media studied while, these constants have higher values than the *f(νP-O)*, as expected due to the lower P=O distances values. The ionic characteristics of the V-O bonds in the two species justify the high *f(νV-O)* values. On the contrary, for both species, the *f(δO-P-O)* have higher values than the *f(δO=P=O)* and *f(δO-V-O)*, in both media and with all the levels of calculations while for $Na_3V_2(PO_4)_3$, the *f(δP-O-V)* have higher values than those corresponding to the anion. The higher values for *f(δO-P-O)* are attributed to the lower angles values as consequence of the rings formed by O-P-O angles, as can be seen in Figure 1 and TABLE 1. Note that in $Na_3V_2(PO_4)_3$ the *f(νNa-O)* have higher values in both media and with all the levels of calculations than *f(νP-Na)* because the O atom is most electronegative than the P atom and for this reason, the Na-O bond is most ionic than P-Na bond. As a consequence, the values for the *f(δNa-O-Na)* are higher than the *f(δP-O-Na)*. The presence of three Na^+ ions in $Na_3V_2(PO_4)_3$ increasing the *f(δP-O-V)* force constants values as compared with the corresponding anion due to the lower P-O-V angles values.

CONCLUSIONS

The theoretical molecular structures of $Na_3V_2(PO_4)_3$ and their anion were determined in gas and aqueous solution phases by using HF, B3LYP and B3P86 methods and the LanL2DZ and CEP-4G basis sets. The structural and vibrational properties for the anion were performed in gas phase by using the combination B3LYP/LanL2DZ while in solution the adequate approximation was B3LYP/CEP-4G. The calculated harmonic vibrational frequencies by using the B3LYP/LanL2DZ and B3P86/LanL2DZ methods for the compound are consistent with the available experimental IR spectrum. The corresponding force fields for the two levels of theory were obtained in both media together with their complete vibrational assignments. The vibrational analyses for both species suggest the noTABLE influence of the Na^+ ions on the vibration modes of the PO_4 groups in both studied media. The predicted Raman spectrum for $Na_3V_2(PO_4)_3$ at the B3LYP/LanL2DZ level was reported. Probably the increase of the molar volumes observed for the two species in solution as consequence of the hydration justify the higher movilities of the Na^+ ions in the three-dimensional framework. The solvation energies for $Na_3V_2(PO_4)_3$ and their anion by using the B3LYP/LanL2DZ level are -384.15 and -1561.64 kJ/mol, respectively. The bond orders predict for the V atoms of the anion a coordination (III) and a coordination (V) in $Na_3V_2(PO_4)_3$ while the maps electrostatic potential show that the sodium and vanadium cations are coordinated to the PO_4 anions, as reported experimentally. The NBO and AIM studies reveals the high stability of $Na_3[V_2(PO_4)_3]$ and their anion attributed to the presence of covalent, ionic and of H bonds interactions in the compound and, to the covalent and ionic interactions in the anion.

ACKNOWLEDGEMENTS

This work was funded with grants from CIUNT (Consejo de Investigaciones, Universidad Nacional de Tucumán). The authors thank Prof. Tom Sundius for his permission to use MOLVIB.

Supporting information available

TABLES S1-S22 and Figures S1-S5 are the supporting information.

REFERENCES

[1] W.Song, X.Ji, Y.Zhu, H.Zhu, F.Li, J.Chen, F.Lu, Y.Yao, C.E.Banks; *Chem.Electro.Chem*, **1(5)**, 819-956 **(2014)**.

[2] J.Liu, K.Tang, K.Song, P.A.van Aken, Y.Yu, J.Maier; Nanoscale, **6(10)**, 5081-5086 **(2014)**.

[3] W.Song, X.Ji, Y.Yao, H.Zhu, Q.Chen, Q.Sun, C.E.Banks; Phys.Chem.Chem.Phys., **16,** 3055-3061 **(2014)**.

[4] R.A.Shakoor, D.H.Kim, Y.U.Park, J.Kim, S.W.Kim, H.Gwon, S.Lee, K.Kang; J.Mat.Chem., **22(38)**, 20535-20541 **(2012)**.

[5] I.V.Zatovsky; NASICON-type $Na_3V_2(PO_4)_3$, Acta Cryst., **E66**, i12 **(2010)**.

ORIGINAL ARTICLE

[6] C.M.Burba; Vibrational spectroscopy of phosphate-based electrodes for lithium rechargeable batteries, Thesis, University of Oklahoma, Norman, Oklahoma, **(2006)**.

[7] L.C.Bichara, M.V.Fiori Bimbi, C.A.Gervasi, P.E.Alvarez, S.A.Brandán; J.Mol.Struct., **1008**, 95-101 **(2012)**.

[8] C.Gervasi, P.Palacios, P.Alvarez, M.Fiori-Bimbi, S.A.Brandán; Industrial & Engineering Chemistry Res., **52**, 9115-9120 **(2013)**.

[9] H.A.Höppe, K.Kazmierczak, E.Romano, S.A.Brandán; J.Mol.Struct., **1037**, 294-300 **(2013)**.

[10] E.Romano, L.Davies, S.A.Brandán; J.Mol.Struct., **1044**, 144-151 **(2013)**.

[11] S.A.Brandán; A structural and vibrational investigation into chromylazide, Acetate, Perchlorate, and Thiocyanate Compounds, Editado by Ken Derham, Springer Science, Business Media B.V., Van Godewijckstraat 30, 3311 GZ Dordrecht, Netherlands.ISBN: 978-94-007-5753-0 (Print) 978-94-007-5754-7 (Online), **(2012)**.

[12] S.A.Brandán; A Structural and vibrational study of the chromyl chlorosulfate, Fluorosulfate, and Nitrate Compounds, Editado by Ken Derham, Springer Science, Business Media B.V., Van Godewijckstraat 30, 3311 GZ Dordrecht, Netherlands.ISBN: 978-94-007-5762-2 (Print) 978-94-007-5763-9 (Online), **(2012)**.

[13] P.Pulay, G.Fogarasi, F.Pang, E.Boggs; J.Am.Chem.Soc., **101(10)**, 2550 **(1979)**.

[14] P.J.Hay, W.R.Wadt; J.Chem.Phys., **82**, 270 **(1985)**.

[15] W.R.Wadt, P.J.Hay; J.Chem.Phys., **82**, 284 **(1985)**.

[16] P.J.Hay, W.R.Wadt; J.Chem.Phys., **82**, 299 **(1985)**.

[17] W.J.Stevens, H.Basch, M.Krauss; J.Chem.Phys., **81**, 6026-6033 **(1984)**.

[18] W.J.Stevens, M.Krauss, H.Basch, P.G.Jasien; Can.J.Chem., **70**, 612-630 **(1992)**.

[19] T.R.Cundari, W.J.Stevens; J.Chem.Phys., **98**, 5555-5565 **(1993)**.

[20] J.Tomasi, Persico; Chem.Rev., **94**, 2027-2094 **(1994)**.

[21] C.Socolsky, S.A.Brandán, A.Ben Altabef, E.L.Varetti; J.Mol.Struct., **672(1-3)**, 45-50 **(2004)**.

[22] M.L.Roldán, H.Lanús, S.A.Brandán, J.J.López, E.L.Varetti, A.Ben Altabef; J.Argent.Chem.Soc., **92(1/3)**, 53-61 **(2004)**.

[23] M.Fernández Gómez, A.Navarro, S.A.Brandán, C.Socolsky, A.Ben Altabef, E.L.Varetti; J.Mol.Struct., **626**, 101-111 **(2003)**.

[24] S.A.Brandán; J.Mol.Struc.(THEOCHEM), **908**, 19-25 **(2009)**.

[25] M.L.Roldán, S.A.Brandán, E.L.Varetti, A.Ben Altabef; Z.Anorg.Allg.Chem., **632**, 2495-2499 **(2006)**.

[26] S.A.Brandán, C.Socolsky, A.Ben Altabef; Z.Anorg.Allg.Chem., **635(3)**, 582-592 **(2009)**.

[27] S.Bell, T.J.Dines; J.Phys.Chem.A, **104**, 11403 **(2000)**.

[28] A.D.Becke; J.Chem.Phys., **98**, 5648–5652 **(1993)**.

[29] C.Lee, W.Yang, R.G.Parr; Phys.Rev., **B37**, 785–789 **(1988)**.

[30] A.B.Nielsen, A.J.Holder, Gauss View 3.0, User's Reference, Gaussian Inc., Pittsburgh, PA, **(2003)**.

[31] M.J.Frisch, G.W.Trucks, H.B.Schlegel, G.E.Scuseria, M.A.Robb, J.R.Cheeseman, J.A.Jr.Montgomery, T.Vreven, K.N.Kudin, J.C.Burant, J.M.Millam, S.S.Iyengar, J.Tomasi, V.Barone, B.Mennucci, M.Cossi, G.Scalmani, N.Rega, G.A.Petersson, H.Nakatsuji, M.Hada, M.Ehara, K.Toyota, R.Fukuda, J.Hasegawa, M.Ishida, T.Nakajima, Y.Honda, O.Kitao, H.Nakai, M.Klene, X.Li, J.E.Knox, H.P.Hratchian, J.B.Cross, C.Adamo, J.Jaramillo, R.Gomperts, R.E.Stratmann, O.Yazyev, A.J.Austin, R.Cammi, C.Pomelli, J.W.Ochterski, P.Y.Ayala, K.Morokuma, G.A.Voth, P.Salvador, J.J.Dannenberg, V.G.Zakrzewski, S.Dapprich, A.D.Daniels, M.C.Strain, O.Farkas, D.K.Malick, A.D.Rabuck, K.Raghavachari, J.B.Foresman, J.V.Ortiz, Q.Cui, A.G.Baboul, S.Clifford, J.Cioslowski, B.B.Stefanov, G.Liu, A.Liashenko, P.Piskorz, I.Komaromi, R.L.Martin, D.J.Fox, T.Keith, M.A.Al-Laham, C.Y.Peng, A.Nanayakkara, M.Challacombe, P.M.W.Gill, B.Johnson, W.Chen, M.W.Wong, C.Gonzalez, J.A.Pople; Gaussian 09, Revision A.02, Gaussian, Inc.: Pittsburgh, PA, **(2009)**.

[32] A.V.Marenich, C.J.Cramer, D.G.Truhlar; J.Phys.Chem., **B113**, 6378-6396 **(2009)**.

[33] L.L.Zhang, G.Liang, A.Ignatov, M.C.Croft, X-Q.Xiong, I-M.Hung, Y-H.Huang, X-L.Hu, W-X.Zhang, Y-L.Peng; J.Phys.Chem.C, **115**, 13520–13527 **(2011)**.

[34] E.D.Glendening, J.K.Badenhoop, A.D.Reed, J.E.Carpenter, Weinhold; F.NBO 3.1, Theoretical Chemistry Institute, University of Wisconsin; Madison, WI, **(1996)**.

[35] L.Wang, K.Zhang, Z.Hu, W.Duan, F.Cheng; J.Chen, Nano Research, **7(2)**, 163-170 **(2014)**.

[36] M.P.Maldonado Manso, Preparación; Cristaloquímica y comportamiento eléctrico de

electrolitos sólidos de estequiometría NASICON, Thesis, Universidad de Málaga, Málaga, España, **(2004)**.

[37] Rajesh Tripathi; Novel High Voltage Electrodes for Li-ion Batteries, Thesis, University of Waterloo, Ontario, Canada, **(2013)**.

[38] R.F.W.Bader; Atoms in Molecules, A quantum theory, Oxford university press, Oxford, ISBN: 0198558651, **(1990)**.

[39] F.Biegler-Köning, J.Schönbohm, D.Bayles; J.Comput.Chem., **22**, 545 **(2001)**.

[40] Ugliengo; P.MOLDRAW Program, University of Torino, Dipartimento Chimica IFM, Torino, Italy, **(1998)**.

[41] T.Sundius; Vib.Spectrosc., **29**, 89-95 **(2002)**.

[42] M.L.Roldán, A.E.Ledesma, A.B.Raschi, M.V.Castillo, E.Romano, S.A.Brandán; J.Molec.Struct., **1041**, 73-81 **(2013)**.

[43] I.S.Bushmarinov, K.A.Lyssenko, M.Yu Antipin; Russian Chem.Rev., **78(4)**, 283-302 **(2009)**.

[44] R.G.Parr, R.G.Pearson; J.Am.Chem.Soc., **105**, 7512-7516 **(1983)**.

[45] S.A.Brandán, S.B.Díaz, R.Cobos Picot, E.A.Disalvo, A.Ben Altabef; Spectrochimica Acta Part A, **66**, 1152-1164 **(2007)**.